

## $(d, p)$ reactions on $^{124}\text{Sn}$ , $^{130}\text{Te}$ , $^{138}\text{Ba}$ , $^{140}\text{Ce}$ , $^{142}\text{Nd}$ , and $^{208}\text{Pb}$ below and near the Coulomb barrier

A. Strömich,\* B. Steinmetz,\* R. Bangert, B. Gonsior,† M. Roth,† and P. von Brentano

*Institut für Kernphysik der Universität zu Köln, † Köln, Germany*

(Received 24 January 1977; revised manuscript received 4 August 1977)

The reactions  $^{124}\text{Sn}(d, p)^{125}\text{Sn}$ ,  $^{130}\text{Te}(d, p)^{131}\text{Te}$ ,  $^{138}\text{Ba}(d, p)^{139}\text{Ba}$ ,  $^{140}\text{Ce}(d, p)^{141}\text{Ce}$ ,  $^{142}\text{Nd}(d, p)^{143}\text{Nd}$ , and  $^{208}\text{Pb}(d, p)^{209}\text{Pb}$  have been investigated by measuring the differential cross sections of the  $(d, p)$  reactions and of the elastic scattering of deuterons at various incident energies below and near the Coulomb barrier. Using scattering potentials which describe the elastic scattering of the particles in the entrance and exit channels, reduced normalizations of 40 final states have been determined which are nearly independent of the uncertainties due to the ambiguities of optical potentials. The experimental errors are 8% on the average. In the energy region studied the expected constancy of derived spectroscopic factors is demonstrated.

NUCLEAR REACTIONS  $^{124}\text{Sn}$ ,  $^{130}\text{Te}$ ,  $^{138}\text{Ba}$ ,  $^{140}\text{Ce}$ ,  $^{142}\text{Nd}$ ,  $^{208}\text{Pb}(d, p)$ ,  $(d, d)$ ,  $5.0 \text{ MeV} \leq E_d \leq 11.0 \text{ MeV}$ , measured  $d\sigma/d\Omega(E_d, \theta)$ , enriched targets, deduced scattering potentials, reduced normalizations of 40 final states with experimental errors of 8% on the average, spectroscopic factors.

### I. INTRODUCTION

A serious problem in the distorted wave Born approximation (DWBA) analysis of the  $(d, p)$  reactions in the energy region several MeV above the Coulomb barrier is the fact that the parameters of the optical potentials describing the elastic scattering of deuterons and protons cannot be determined uniquely.<sup>1,2</sup> As cross sections calculated with DWBA at those energies depend sensitively on the optical potentials, the extracted spectroscopic factors (SF) are at best accurate to only about  $\pm 30\%$ .

The influence of the optical potentials on the scattering wave functions is much less pronounced if the energies of the incoming and outgoing particles are well below the Coulomb barriers. According to theoretical investigations and calculations<sup>3</sup> in this region of "sub-Coulomb stripping,"<sup>3-5</sup> the SF can be extracted much more accurately. As Smith<sup>6</sup> and von Brentano, Dost, and Harney<sup>7</sup> have shown, one expects to obtain almost the same accuracy in the energy region of "quasi-Coulomb stripping," i.e., near the Coulomb barrier. In that case one needs optical potentials reproducing the elastic scattering data of deuterons and protons at energies occurring in the entrance and exit channels of the stripping reactions. Nevertheless, the SF determined from sub-Coulomb and quasi-Coulomb stripping still remain dependent on special assumptions about shape and geometry of the bound neutron potential. The reduced normalization  $\Lambda$  is a quantity which is nearly independent of models and geometries.

The determination of the SF or  $\Lambda$  with high accuracy is interesting for a meaningful comparison of SF or  $\Lambda$  resulting from both  $(d, p)$  stripping reactions and elastic proton scattering via analog resonances. Such comparison is important for testing various theories of analog resonances.

Careful measurements and analysis have been done at analog resonances in  $^{125}\text{Sb}$ ,  $^{131}\text{I}$ ,  $^{139}\text{La}$ ,  $^{141}\text{Pr}$ ,  $^{143}\text{Pm}$ , and  $^{209}\text{Bi}$ .<sup>8-24</sup> Therefore, the aim of this work was to determine reduced normalizations  $\Lambda$  of the corresponding parent states by measuring and analyzing  $(d, p)$  reactions in the sub-Coulomb and quasi-Coulomb region. Previous measurements of the  $(d, p)$  stripping reactions for these nuclei at higher bombarding energies<sup>25-36</sup> only provide SF affected with the above mentioned problems. Furthermore, up to now the interpretations of measurements at quasi-Coulomb and sub-Coulomb energies<sup>34-42</sup> suffer in most cases from large experimental errors due to the difficulties in the determination of the absolute cross sections and due to impurities in the targets.

In this paper we first give a short review of the theory of sub-Coulomb stripping. Then we will describe the experiments and discuss the errors made in obtaining reduced normalizations. We compare our results with other measurements, in particular with the work by Rapaport and Kerman<sup>39</sup> and by Norton *et al.*<sup>40</sup>

### II. $(d, p)$ STRIPPING REACTION AT LOW ENERGIES

The DWBA theory of stripping reactions at various incident energies has been reviewed in many

papers,<sup>1-7</sup> so we will only write down some formulas and introduce some concepts which we will use later on. The experimental differential cross section of the reaction  $A(d, p)B$  from a spin 0 target nucleus  $A$  is usually fitted by a theoretical DWBA single particle cross section  $\sigma_{ij}^{\text{DWBA}}$  and a spectroscopic factor  $S_{ij}$

$$\frac{d\sigma^{\text{exp}}}{d\Omega} = (2J_B + 1)S_{ij}\sigma_{ij}^{\text{DWBA}}. \quad (1)$$

At incident energies below the Coulomb barrier the reaction takes place outside the nucleus. In this case the reaction samples only the asymptotic part of the bound state wave function. It is then advantageous to replace the spectroscopic factor by the asymptotic normalization  $\Lambda_{ij}$  of the bound state neutron wave function  $u_{ij}(r)$  which is defined by

$$u_{ij}(r) = \langle B|A \rangle \\ = [(2J_B + 1)\Lambda_{ij}]^{1/2} k_B^{-3/2} i^{-1} h_1^{(-)}(ik_B r), \quad (2)$$

for  $r \gg R_n$ ,

where  $E_B = (\hbar k_B)^2 / 2\mu_n$  and  $\mu_n$  are the binding energy and reduced mass of the neutron, respectively. The asymptotic normalization  $\Lambda_{ij}$  is related to the spectroscopic factor  $S_{ij}$ :

$$\Lambda_{ij} = S_{ij}\Lambda_{ij}^{\text{sp}}. \quad (3)$$

The normalization  $\Lambda_{ij}^{\text{sp}}$  has been computed from Eq. (2) by taking  $u_{ij}(r)$  to be the wave function  $u_{ij}^{\text{sp}}(r)$  of a single neutron in a Woods-Saxon well with binding energy  $E_B$ . The reason for the advantages of  $\Lambda_{ij}$  as opposed to  $S_{ij}$  is that  $\Lambda_{ij}^{\text{sp}}$  and  $\sigma_{ij}^{\text{DWBA}}$  depend very sensitively on the radius of the Woods-Saxon well, whereas  $(1/\Lambda_{ij}^{\text{sp}})\sigma_{ij}^{\text{DWBA}}$  is nearly independent. Thus it is reasonable to factorize  $d\sigma^{\text{exp}}/d\Omega$  in the form

$$\frac{d\sigma^{\text{exp}}}{d\Omega} = (2J_B + 1)\Lambda_{ij} \left( \frac{1}{\Lambda_{ij}^{\text{sp}}} \sigma_{ij}^{\text{DWBA}} \right). \quad (4)$$

The use of  $\Lambda_{ij}$  extends clearly from the pure Coulomb stripping case to quasi-Coulomb stripping. It is a reasonable quantity to compare various ex-

periments even at higher energies.

In the literature it is customary to analyze the data to give the spectroscopic factor  $S_{ij}$  rather than the asymptotic normalization  $\Lambda_{ij}$ . For sub-Coulomb stripping, as we have pointed out,  $\Lambda_{ij}$  is the more directly determined quantity and  $S_{ij}$  is a derived one [by help of Eq. (4) and a computation of  $\Lambda_{ij}$ , which is very dependent on the potential geometry of the bound neutron]. In the following we will give both quantities, but we will attach importance only to  $\Lambda_{ij}$ . Thus we will not care about the fulfillment of sum rules for  $S_{ij}$  as a small change in the potential geometry of the bound neutron allows us to change the extracted  $S_{ij}$  very much. Also we analyzed the data using the best optical potentials available for the various elements, though this also implied a change of the potential geometry from element to element for the bound state. We stress once more the fact which will be demonstrated below that  $\Lambda_{ij}$  as extracted from experiment using Eq. (4) is rather insensitive to changes in the potential geometry of the bound states (although it depends probably via the scattering phases on changes in the optical potentials for elastic scattering). These questions will be extensively discussed in Sec. VI.

### III. EXPERIMENT

An important criterion of the quality of the extracted SF and reduced normalizations is their energy independence. Therefore, the  $(d, p)$  reactions have been investigated at various energies below and near the Coulomb barrier. Table I gives a summary of the reactions, the incident energies, the  $Q$  values of the ground state transitions, and the heights of the Coulomb barriers in the incoming and outgoing channels.

The differential  $(d, p)$  cross sections for medium and heavy target nuclei in the energy region of sub-Coulomb and quasi-Coulomb stripping are of the order of  $\mu\text{b}/\text{sr}$ . Therefore, and because of the unavoidable presence of light nuclei in the targets, good detector resolution and low background in the

TABLE I. Reactions investigated, incident deuteron energies,  $Q$  values of the ground state transitions, and Coulomb barrier heights for deuterons and protons [ $R_d = 2.80$  fm,  $R_p = 1.034$  fm,  $R_A = 1.20A^{1/3}$  fm (Ref. 44)].

Reaction	$E_d$ (MeV)	$Q$ (MeV)	$E_d^c$ (MeV)	$E_p^c$ (MeV)
$^{124}\text{Sn}(d, p)^{125}\text{Sn}$	5.0, 6.0, 7.0, 8.0	3.534	8.2	10.2
$^{130}\text{Te}(d, p)^{131}\text{Te}$	5.0, 6.0, 7.0, 8.5	3.703	8.4	10.5
$^{138}\text{Ba}(d, p)^{139}\text{Ba}$	5.0, 6.0, 7.0, 8.5	2.494	9.0	11.1
$^{140}\text{Ce}(d, p)^{141}\text{Ce}$	5.0, 6.0, 7.0, 8.5	3.214	9.3	11.5
$^{142}\text{Nd}(d, p)^{143}\text{Nd}$	5.0, 6.0, 7.0, 8.5	3.916	9.5	12.0
$^{208}\text{Pb}(d, p)^{209}\text{Pb}$	7.0, 8.0, 9.0, 10.0, 11.0	1.708	11.9	14.5

TABLE II. Characteristics of the targets.

Target	Enrichment (%)	Target material	Backing
$^{124}\text{Sn}$	95.3	Sn	No
$^{130}\text{Te}$	99.49	Te	Carbon
$^{138}\text{Ba}$	99.1	$\text{BaCO}_3$	Carbon
$^{140}\text{Ce}$	99.7	$\text{CeO}_2$	Carbon
$^{142}\text{Nd}$	98.26	Nd	Carbon
$^{208}\text{Pb}$	99.96	Pb	No

spectra are very important. Without collimation more than 99% of the deuteron beam of the FN tandem Van de Graaff accelerator of the Universität zu Köln was focused onto a spot 2 mm in diameter in the center of a 76-cm ORTEC 2800 scattering chamber. Using a rotating target holder,<sup>43</sup> the beam current could be raised to about 800 nA even for Te and Pb targets. Targets of thicknesses of about 100 to 200  $\mu\text{g}/\text{cm}^2$  were made by high vacuum evaporation. Table II gives their principal characteristics.

The charged particles emerging from the target have been measured with four silicon surface barrier detectors placed at the lab angles  $50^\circ$ ,  $90^\circ$ ,  $140^\circ$ , and  $170^\circ$ . By cooling the detectors to 240 K and by deflecting secondary electrons with two horseshoe-shaped magnets in front of each detector, a resolution of 15 keV could be achieved. Since the proton peaks of the investigated  $(d, p)$  reactions are in most cases energetically well above the peaks of the elastically scattered deuterons, we could evade particle discrimination.

The pulse height analyzer system consisted of a Victoreen analog to digital converter (ADC) with  $4 \times 1024$  memory and of a Tennelec ADC with  $4 \times 2048$  memory of a PDP9 computer. Dead time correction was made using a fast counter system.

Figure 1 shows examples of the measured particle spectra. For better orientation the excitation energies of some prominent  $(d, p)$  peaks as well as the  $(d, d_0)$  peaks at the target nuclei and  $(d, p)$  peaks of some contaminant nuclei are indicated in these figures.

The spectra have been analyzed on a PDP9 16384 computer by fitting modified Gaussian distributions with low energy tails to the peaks of interest. The parameters of these distributions were taken from fits to the  $(d, d_0)$  and other prominent peaks of the particular spectrum. In the case of overlapping peaks up to three lines could be resolved.<sup>45</sup>

#### IV. ABSOLUTE CROSS SECTIONS

Absolute differential cross sections were obtained by normalizing the counting rates to the yields of the elastic deuteron scattering measured

symmetrically to the beam direction at  $\theta_{\text{lab}} = \pm 50^\circ$ .

According to this method the differential cross section of the  $(d, p)$  reaction at lab energy  $E_d$  and lab angle  $\theta$  is given by the relation

$$\frac{d\sigma}{d\Omega}(E_d, E_x, \theta) = \frac{d\sigma_{\text{el}}}{d\Omega}(E_d, 50^\circ) \frac{\Delta\Omega(50^\circ)}{\Delta\Omega(\theta)} \times \frac{N(E_d, E_x, \theta)}{N_{\text{el}}(E_d, 50^\circ)}, \quad (5)$$

where  $d\sigma/d\Omega(E_d, E_x, \theta)$  is the  $(d, p)$  cross section leading to the final state with the excitation energy  $E_x$ ;  $d\sigma_{\text{el}}/d\Omega(E_d, 50^\circ)$  is the theoretical differential cross section of the elastic deuteron scattering, which at the chosen energies is almost pure Rutherford scattering;  $\Delta\Omega(50^\circ)/\Delta\Omega(\theta)$  is the ratio of the solid angles of the detectors;  $N(E_d, E_x, \theta)$  is the experimental yield of the  $(d, p)$  reaction to the state  $E_x$ ; and  $N_{\text{el}}(E_d, 50^\circ)$  are the counts of the elastically scattered deuterons at  $\Theta_{\text{lab}} = 50^\circ$  which were measured simultaneously. There are some advantages of this normalization method: Errors due to small deviations of the deuteron beam from the center of the scattering chamber or small changes of the angle of incidence of the beam are almost negligible; inhomogeneities or changes of the target thickness do not influence the results; measurements of beam charge and target thickness and an absolute determination of the solid angles of the detectors are not necessary.

The cross sections  $d\sigma/d\Omega(E_d, 50^\circ)$  were calculated with the computer code MOM3<sup>46</sup> using optical potentials determined by other authors,<sup>25,29,35,38,39</sup> mostly at higher energies. At the highest incident energies of our work the part of the cross section due to the scattering by the nuclear potential alone is 5%. Therefore, it is sufficient to take approximate values of the potential parameters.

The solid angle ratios  $\Delta\Omega(50^\circ)/\Delta\Omega(\Theta)$  were obtained by measuring the reaction  $^{130}\text{Te}(p, p_0)$  at  $E_p = 9$  MeV and  $\Theta = 150^\circ$ , with each of the detectors. Since the cross section for this reaction varies only slightly with energy and angle,<sup>13</sup> small changes in energy and angle during this procedure are of negligible influence on the measured solid angle ratios.

The determination of absolute cross sections described above reduces considerably the systematic error. The errors in  $d\sigma/d\Omega(E_d, 50^\circ)$  were estimated by varying the parameters of the optical potentials and are within 2%. There is a peak fitting error due to the deviations of the actual peak shape from the distribution described by best fit parameters (cf. Sec. III), which is also within 2%. The errors caused by geometrical uncertainties of the target position, the aperture position, and the angle adjustment in the scattering chamber sum up to 1%. These independent errors have

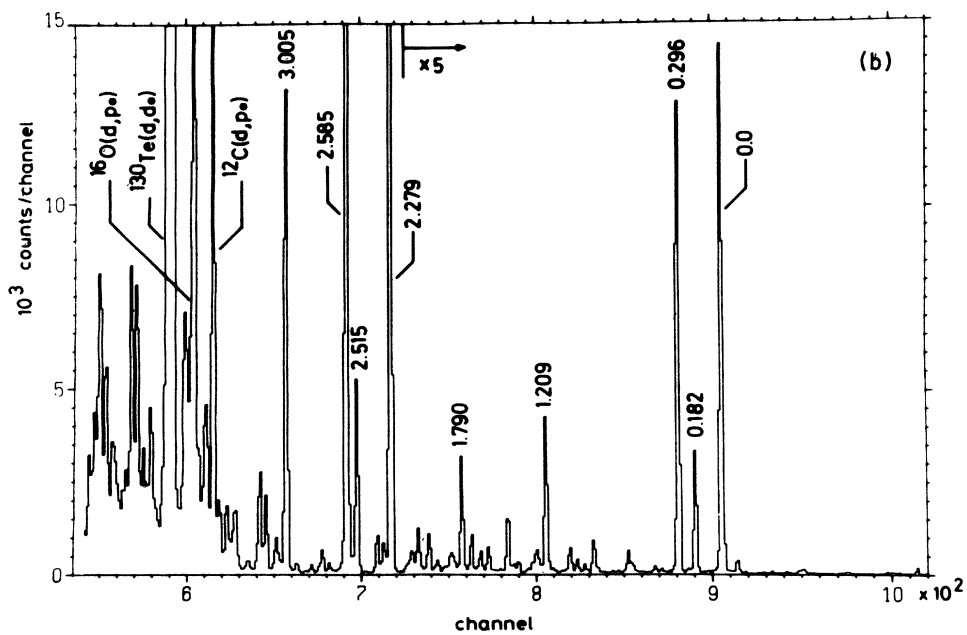
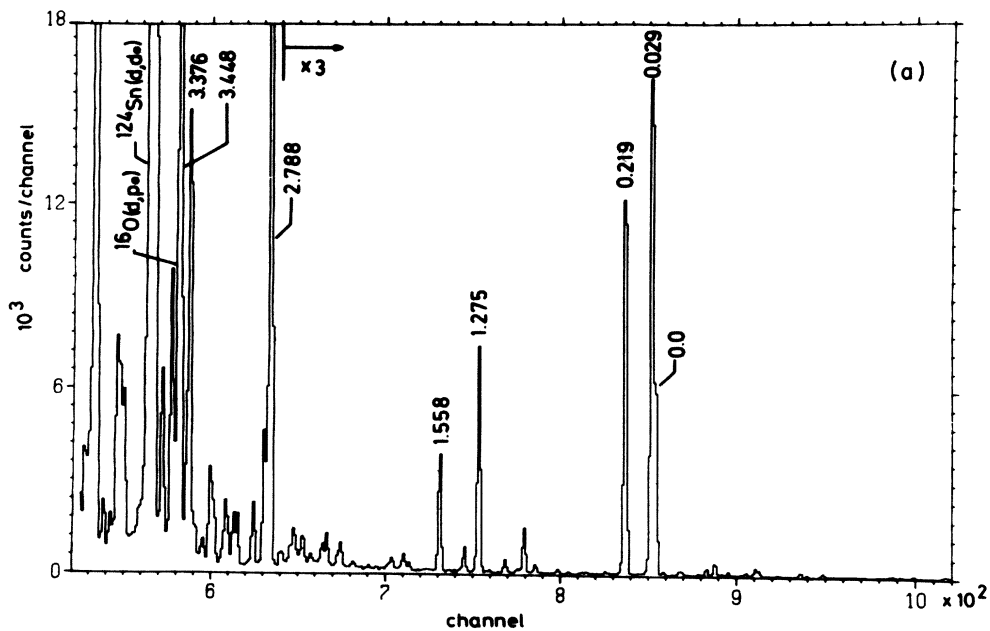


FIG. 1. Particle spectra. (a)  $^{124}\text{Sn}$  target,  $E_d = 7.0$  MeV,  $\Theta = 140^\circ$ ; (b)  $^{130}\text{Te}$  target,  $E_d = 7.0$  MeV,  $\Theta = 140^\circ$ ; (c)  $^{138}\text{Ba}$  target,  $E_d = 7.0$  MeV,  $\Theta = 140^\circ$ ; (d)  $^{140}\text{Ce}$  target,  $E_d = 7.0$  MeV,  $\Theta = 140^\circ$ ; (e)  $^{142}\text{Nd}$  target,  $E_d = 7.0$  MeV,  $\Theta = 140^\circ$ ; (f)  $^{208}\text{Pb}$  target,  $E_d = 9.0$  MeV,  $\Theta = 140^\circ$ .

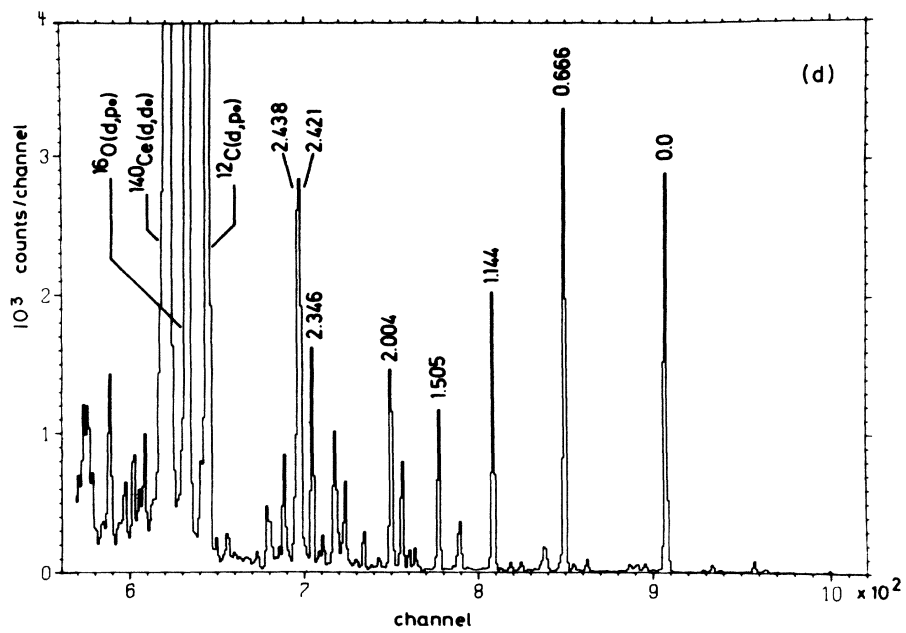
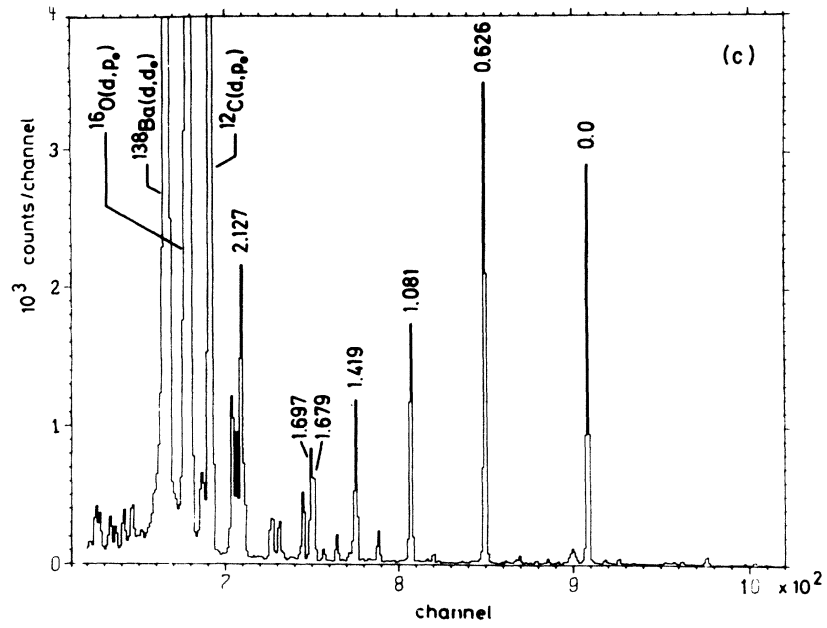


FIG. 1. (continued)

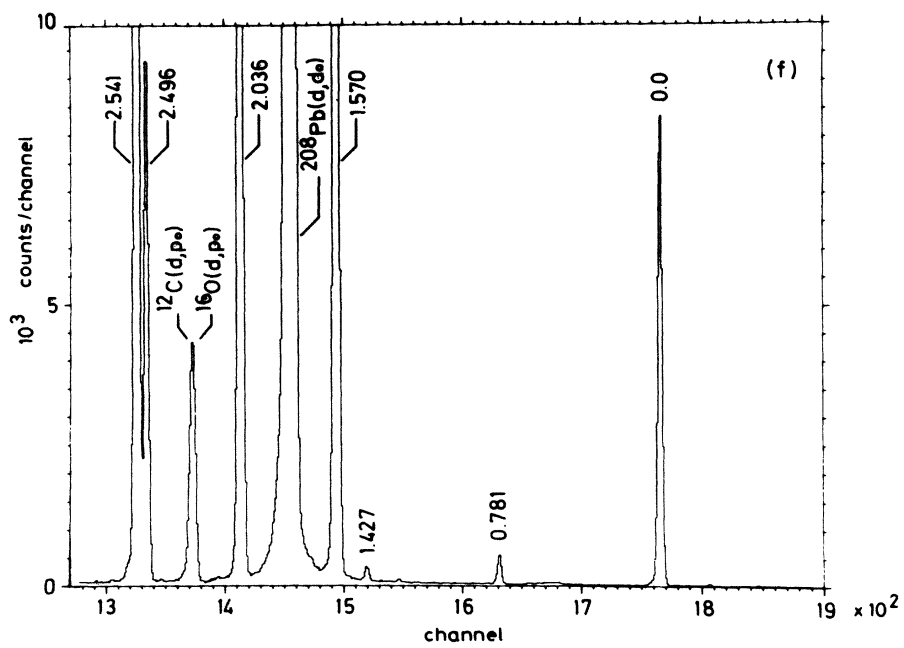
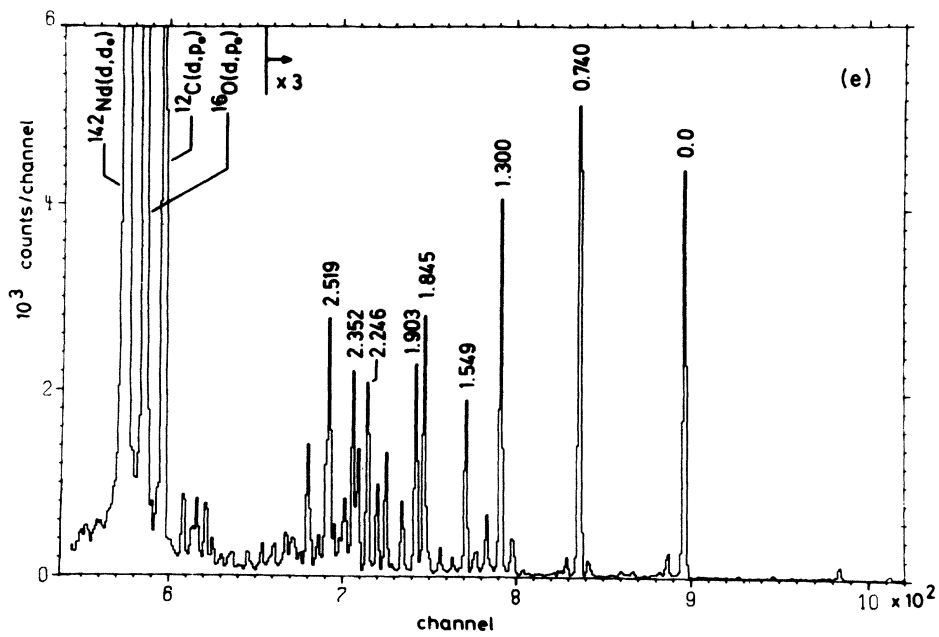


FIG. 1. (continued)

been added linearly to give a total systematic error of 5%. All the other errors which have to be considered in Eq. (5) result from intensity measurements. They have been added quadratically to give the total statistical error.

Absolute differential cross sections of the elastic deuteron scattering have been determined in the same way as the (d, p) cross sections. However, the (d,  $d_0$ ) peaks have been fitted using free peak shape parameters. Hence, the systematic errors of the elastic differential cross sections are only 3%, which are made up of the remaining uncertainties in the apparatus geometry and in the optical potentials used in calculating  $d\sigma/d\Omega(E_d, 50^\circ)$ . Of course, the statistical error of the elastic yields was added to give the total error.

### V. ANALYSIS

The complete DWBA analysis of (d, p) reactions requires two complex nuclear potentials acting on the particles in the entrance and exit channels and a real potential determining the bound neutron wave function. These potentials are specified in the Secs. VA and VB below.

The theoretical (d, p) cross sections were calculated with the DWBA code DWUCK<sup>47</sup> using the zero-range approximation and local potentials. Using the computer code BETTINA,<sup>48</sup> we obtained the reduced normalizations of the neutron single particle states  $\Lambda_{ij}^n$ . Section VC provides the spectroscopic quantities  $S_{ij}$  and  $\Lambda_{ij}$  and some resulting energy and angular distributions.

#### A. Optical potentials

The potentials used in this work to describe the elastic scattering are chosen to have the following form:

$$U(r) = U_R(r) + iU_I(r) + U_S(r) + U_C(r) \quad (6)$$

with

$$U_R(r) = -V_R f(r, R_R, a_R), \quad \text{volume potential,}$$

$$U_I(r) = 4a_I W_D \frac{d}{dr} f(r, R_I, a_I), \quad \text{surface potential,}$$

$$U_S(r) = V_S (\vec{\sigma} \cdot \vec{l}) (\hbar/m_\pi c)^2 \frac{1}{r} \frac{d}{dr} f(r, R_S, a_S), \quad \text{spin-orbit potential,}$$

$$U_C(r) = \begin{cases} \frac{Ze^2}{2R_C} \left( 3 - \frac{r^2}{R_C^2} \right), & r \leq R_C \\ \frac{Ze^2}{r}, & r \geq R_C, \end{cases} \quad \text{Coulomb potential,}$$

where  $V_R$ ,  $W_D$ , and  $V_S$  are the potential depths,  $f(r, R_x, a_x) = \{1 + \exp[(R - R_x)/a_x]\}^{-1}$  determines the Woods-Saxon form of the potentials,  $R_x = r_x A^{1/3}$  are the radii, and  $a_x$  the diffusenesses of the vari-

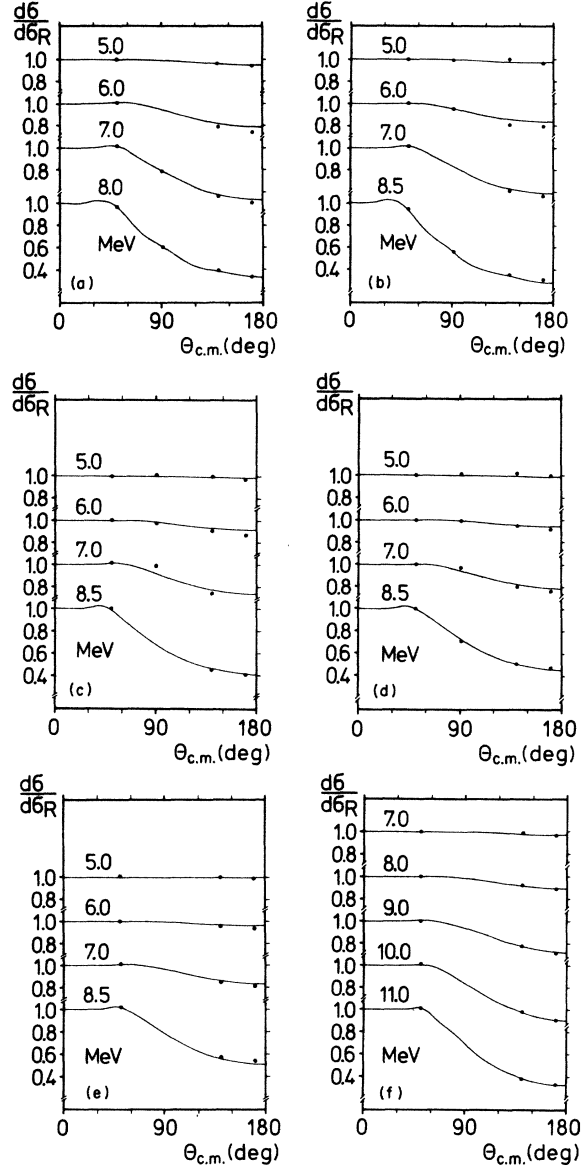


FIG. 2. Angular distributions of the elastic deuteron scattering. The solid curves are the best fits using the parameters in Table III. (a)  $^{124}\text{Sn}$  (d,  $d_0$ ); (b)  $^{130}\text{Te}$  (d,  $d_0$ ); (c)  $^{138}\text{Ba}$  (d,  $d_0$ ); (d)  $^{140}\text{Ce}$  (d,  $d_0$ ); (e)  $^{142}\text{Nd}$  (d,  $d_0$ ); (f)  $^{208}\text{Pb}$  (d,  $d_0$ ).

ous potentials.  $Z$  is the charge number,  $A$  the mass number of the target nucleus,  $(\vec{\sigma} \cdot \vec{l})$  is the scalar product of the spin operator with the orbital angular momentum operator, and  $m_\pi$  is the pion mass. In the case of elastic deuteron scattering, for the volume depth the relation  $V_R = V_{R0} + K_1 Z/A^{1/3} + K_2 E_d$  as given by Perey and Perey<sup>49</sup> was used. Theoretical distributions of the elastic deuteron scattering were fitted to the experimental data using the optical potential parameter search code MOM3<sup>46</sup> (cf. Fig. 2). This code, in contrast to

TABLE III. Optical potentials used in the DWBA analysis.

Nucleus	$V_R$ (MeV)	$W_D$ (MeV)	$V_S$ (MeV)	$r_R$ (fm)	$r_I$ (fm)	$r_S$ (fm)	$r_C$ (fm)	$a_R$ (fm)	$a_I$ (fm)	$a_S$ (fm)
Deuteron parameters										
$^{124}\text{Sn}$	125.8-0.5 $E_d$	16.7-0.25 $E_d$	7.8	1.160	1.350	1.160	1.200	0.840	0.730	0.840
$^{130}\text{Te}$	126.4-0.5 $E_d$	16.7-0.25 $E_d$	7.8	1.160	1.350	1.160	1.200	0.840	0.730	0.840
$^{138}\text{Ba}$	126.4-0.5 $E_d$	20.0-0.25 $E_d$	7.3	1.165	1.330	1.165	1.200	0.800	0.720	0.800
$^{140}\text{Ce}$	126.9-0.5 $E_d$	20.0-0.25 $E_d$	7.3	1.165	1.330	1.165	1.200	0.800	0.720	0.800
$^{142}\text{Nd}$	127.5-0.5 $E_d$	20.0-0.25 $E_d$	7.3	1.165	1.330	1.165	1.200	0.800	0.720	0.800
$^{208}\text{Pb}$	106.5-0.22 $E_d$	8.0-0.25 $E_d$	6.3	1.175	1.250	1.020	1.190	0.710	1.215	0.630
Proton parameters										
$^{125}\text{Sn}^a$	61.6-0.6 $E_p$	13.2	8.5	1.245	1.245	1.245	1.210	0.700	0.700	0.700
$^{131}\text{Te}^b$	63.0-0.5 $E_p$	11.0	7.5	1.22	1.23	1.22	1.25	0.67	0.67	0.67
$^{139}\text{Ba}^c$	63.4-0.4 $E_p$	10.0	5.8	1.230	1.230	1.230	1.230	0.650	0.650	0.650
$^{141}\text{Ce}^d$	63.9-0.6 $E_p$	8.0	6.6	1.230	1.230	1.230	1.230	0.680	0.720	0.680
$^{143}\text{Nd}^e$	64.1-0.6 $E_p$	7.1	3.6	1.230	1.230	1.230	1.200	0.650	0.650	0.650
$^{209}\text{Pb}^c$	66.4-0.4 $E_p$	10.2	5.8	1.19	1.19	1.19	1.19	0.75	0.77	0.75

<sup>a</sup>Fit to data of Ref. 10.<sup>b</sup>Reference 13.<sup>c</sup>Reference 10.<sup>d</sup>Fit to data of Ref. 19.<sup>e</sup>Fit to data of Ref. 22.

other search routines, allows simultaneous fits to the experimental cross sections measured at different angles, energies, and neighboring nuclei. We applied the code simultaneously to the elastic deuteron scattering data of  $^{124}\text{Sn}$  and  $^{130}\text{Te}$ , of  $^{138}\text{Ba}$ ,  $^{140}\text{Ce}$ , and  $^{142}\text{Nd}$ , and of  $^{208}\text{Pb}$ .

The parameters of the deuteron and proton optical potentials used in the DWBA analysis of this work are given in Table III. With the exception of  $^{143}\text{Nd}$ , all the residual nuclei of the reactions studied are unstable. Therefore, the proton potentials were taken from the analysis of the elastic scattering of the target nuclei. They either have been published in the literature or were fitted to data measured by other authors using the program MOM3.

#### B. Bound state neutron potentials

The single particle shell model wave functions are calculated in the codes DWUCK as well as BETTINA according to the usual separation energy method using a real volume and spin-orbit potential with the same geometry as the scattering potentials. With the exception of the volume potential depths, which were adjusted to reproduce the actual binding energies, the parameters were set equal to the values of the appropriate proton potentials given in Sec. VA (cf. Table III).

#### C. Results

DWBA cross sections were calculated only for states with known spins and parities which could be resolved uniquely at several energies and an-

gles. The spectroscopic factors  $S_{ij}$  and reduced normalizations  $\Lambda_{ij}$  of these states were determined at each energy and angle according to Eqs. (1) and (3). The  $S_{ij}$  and  $\Lambda_{ij}$  given in Table IV are the statistical means of the individual values weighted by the reciprocal squared sums of their statistical and instrumental errors. The  $S_{ij}$  in Table IV are also used for normalizing the theoretical angular distributions of some selected states to the experimental data, as shown in Fig. 3.

Furthermore, in Table IV the overall errors of the  $\Lambda_{ij}$  including the systematic and statistical errors and the deviations of the values for different energies and angles from the weighted means are listed. Additional errors of the  $\Lambda_{ij}$  due to uncertainties of the DWBA analysis will be discussed in Sec. VI. They do not exceed  $\pm 5\%$  for the relative values of  $\Lambda_{ij}$  and  $\pm 15\%$  error for the absolute values of  $\Lambda_{ij}$ . As the average error of all  $\Lambda_{ij}$  is about  $\pm 8\%$ , this would lead to a total error of the absolute  $\Lambda_{ij}$  of about  $\pm 25\%$ . We give no errors for the spectroscopic factors because of the problems of the large uncertainties for the correct values of the  $\Lambda_{ij}^{\text{sp}}$ .

Figure 4 presents the extracted  $S_{ij}$  versus the incident deuteron energy. The expected constancy in energy of the SF, and hence of the reduced normalizations, is demonstrated within the indicated error limits. The errors of the  $S_{ij}$  in Fig. 4 were directly deduced from the errors in the  $\Lambda_{ij}$  without allowing any uncertainty in the  $\Lambda_{ij}^{\text{sp}}$ . Since the restriction to a few angles measured with high accuracy is only reasonable in cases of weakly structured angular distributions, the reduced normalizations



TABLE IV. Spectroscopic factors  $S_{IJ}$  and reduced normalizations  $\Lambda_{IJ}$  of the states with excitation energies  $E_x$ , spins and parities  $J^\pi$ , and single particle reduced normalizations  $\Lambda_{ij}^{\text{sp}}$ . The errors quoted comprise all instrumental and statistical errors of the measured cross sections plus the deviations of the single values for different energies from the weighted means. The errors in  $\Lambda_{IJ}$  do not include errors due to the DWBA analysis which we discuss in detail in Sec. VI. These errors on the whole may change the relative values of  $\Lambda_{IJ}$  only by about  $\pm 5\%$ , whereas absolute values can change by about  $\pm 15\%$ . We do not give errors for the SF but the uncertainties can be derived from those for the  $\Lambda_{IJ}$ .

Isotope	$E_x$ (MeV) Error: 0.007	$J^\pi$	$\Lambda_{ij}^{\text{sp}}$	$S_{IJ}$	$\Lambda_{IJ}$
$^{125}\text{Sn}$	0.0	$\frac{11}{2}^-$	0.689	0.34	$0.23 \pm 0.02$
	0.029	$\frac{3}{2}^+$	145.2	0.53	$77.0 \pm 5.0$
	0.219	$\frac{1}{2}^+$	755.3	0.32	$243.0 \pm 21.0$
	2.788	$\frac{7}{2}^-$	5.03	0.52	$2.6 \pm 0.2$
$^{131}\text{Te}$	0.0	$\frac{3}{2}^+$	151.1	0.37	$55.0 \pm 4.0$
	0.182	$\frac{11}{2}^-$	0.588	0.17	$(9.9 \pm 0.8) \times 10^{-2}$
	0.296	$\frac{1}{2}^+$	720.8	0.23	$167.0 \pm 15.0$
	2.279	$\frac{7}{2}^-$	9.17	0.60	$5.5 \pm 0.4$
	2.515	$\frac{3}{2}^-$	138.9	0.065	$9.0 \pm 0.7$
	2.585	$\frac{3}{2}^-$	134.7	0.31	$41.0 \pm 3.0$
	3.005	$\frac{1}{2}^-$	92.4	0.28	$26.0 \pm 2.0$
$^{138}\text{Ba}$	0.0	$\frac{7}{2}^-$	25.5	0.88	$22.0 \pm 2.0$
	0.626	$\frac{3}{2}^-$	236.1	0.52	$123.0 \pm 8.0$
	1.081	$\frac{1}{2}^-$	161.7	0.42	$68.0 \pm 5.0$
	1.283	$\frac{9}{2}^-$	0.0268	0.62	$0.017 \pm 0.002$
	1.419	$\frac{5}{2}^-$	5.58	0.28	$1.6 \pm 0.10$
	1.697	$\frac{5}{2}^-$	4.07	0.17	$0.68 \pm 0.07$
$^{141}\text{Ce}$	0.0	$\frac{7}{2}^-$	50.4	0.85	$43.0 \pm 3.0$
	0.666	$\frac{3}{2}^-$	405.6	0.49	$200.0 \pm 14.0$
	1.144	$\frac{1}{2}^-$	278.5	0.42	$116.0 \pm 9.0$
	1.357	$\frac{9}{2}^-$	$6.85 \times 10^{-2}$	0.64	$(4.4 \pm 0.4) \times 10^{-2}$
	1.505	$\frac{5}{2}^-$	11.4	0.27	$3.1 \pm 0.3$
	1.748	$\frac{7}{2}^-$	11.2	0.095	$1.1 \pm 0.1$
	2.129	$\frac{5}{2}^-$	6.10	0.10	$0.62 \pm 0.05$
	2.421	$\frac{3}{2}^-$	114.0	0.11	$12.0 \pm 1.0$
	2.438	$\frac{1}{2}^-$	106.6	0.22	$24.0 \pm 2.0$
$^{143}\text{Nd}$	0.0	$\frac{7}{2}^-$	77.0	0.85	$66.0 \pm 6.0$
	0.740	$\frac{3}{2}^-$	569.1	0.51	$288.0 \pm 24.0$
	1.300	$\frac{1}{2}^-$	389.0	0.44	$172.0 \pm 13.0$
	1.402	$\frac{9}{2}^-$	0.175	0.59	$0.10 \pm 0.01$
	1.549	$\frac{5}{2}^-$	21.0	0.23	$4.8 \pm 0.4$
	1.845	$\frac{3}{2}^-$	281.2	0.10	$28.0 \pm 2.0$
	1.903	$\frac{5}{2}^-$	15.4	0.22	$3.4 \pm 0.3$

TABLE IV. (Continued)

Isotope	$E_x$ (MeV) Error: 0.007	$J^\pi$	$\Lambda_{IJ}^{np}$	$S_{IJ}$	$\Lambda_{IJ}$
$^{208}\text{Pb}$	0.0	$\frac{9}{2}^+$	5.41	1.21	6.6 $\pm$ 0.5
	0.781	$\frac{11}{2}^+$	$3.56 \times 10^{-3}$	1.57	(5.6 $\pm$ 0.4) $\times 10^{-3}$
	1.427	$\frac{15}{2}^-$	$6.39 \times 10^{-5}$	1.19	(7.6 $\pm$ 0.7) $\times 10^{-5}$
	1.570	$\frac{5}{2}^+$	35.9	1.08	39.0 $\pm$ 2.0
	2.036	$\frac{1}{2}^+$	140.0	1.04	146.0 $\pm$ 9.0
	2.496	$\frac{7}{2}^+$	$5.90 \times 10^{-2}$	1.27	(7.5 $\pm$ 0.5) $\times 10^{-2}$
	2.541	$\frac{3}{2}^+$	7.97	1.11	8.8 $\pm$ 0.6

of the  $\frac{3}{2}^+$  and  $\frac{1}{2}^+$  states in  $^{125}\text{Sn}$  ( $E_x=0.029$  and  $0.211$  MeV) and in  $^{131}\text{Te}$  ( $E_x=0.0$  and  $0.291$  MeV) at deuteron energies of 8.0 and 8.5 MeV were not taken into account.

#### VI. PROBLEMS OF THE ANALYSIS

The problems of the DWBA analysis still remaining in the sub-Coulomb and quasi-Coulomb region are the following:

- (1) The calculated cross sections are not completely independent of the parameters of the nuclear scattering potentials.
- (2) The SF depend on the parameters of the bound neutron potential.
- (3) The remaining influence of the wave functions reaching into the nuclear interior is not known accurately.
- (4) The validity of the approximations in using the zero-range interaction and local potentials is not established.
- (5) The effects of polarization of the deuteron in the Coulomb field of the nucleus are not fully understood.
- (6) There is some uncertainty in the factor  $D_0$  which depends on the  $p$ - $n$  interaction and on the internal wave function of the deuteron.

The assumption often made that the dependence of the theoretical ( $d, p$ ) cross sections on the optical potentials in the quasi-Coulomb region is rather weak and that therefore the choice of global potential parameters should be sufficient, is not justified. This is demonstrated by the following example: DWBA calculations were performed for the reaction  $^{130}\text{Te}(d, p)^{131}\text{Te}$  ( $E_x=2.279$  MeV,  $J^\pi=\frac{7}{2}^-$ ) at  $E_d=5.0, 6.0, 7.0, 8.5$  MeV with the deuteron potential of Perey and Perey<sup>49</sup> [potential A in Table V], used e.g., by Graue *et al.*,<sup>38</sup> as well as with the potential determined in this work (cf. Table III). The resulting cross sections (cf. Fig. 5) and there-

fore the extracted  $S_{IJ}$  differ by as much as 30%. On the other hand, calculations with the parameter sets B and C of Table V lead to spectroscopic factors differing from each other and from the  $S_{IJ}$  given in Table IV by less than 2%. The  $\chi^2$  values of the fits to the measured elastic deuteron scattering data on  $^{124}\text{Sn}$  and  $^{130}\text{Te}$  with the parameter sets B and C agree with the  $\chi^2$  value of the best fit within 3%. The total influence of the nuclear optical potentials was studied at the lowest incident deuteron energy. In this case DWBA calculations using only Coulomb potentials in the entrance and exit channels provide ( $d, p$ ) cross sections which differ from those including the optical potentials by about 10%.

Concerning the second problem, we quoted as an illustration the dependencies of the spectroscopic quantities on the used bound neutron potentials for the ground state ( $J^\pi=\frac{7}{2}^-$ ) and the first excited state ( $E_x=0.626$  MeV,  $J^\pi=\frac{3}{2}^-$ ) in  $^{141}\text{Ce}$ . DWBA calculations with equal radius and diffuseness parameters of the volume and spin-orbit term have been done for a bombarding energy of 6.0 MeV. Figures 6 to 8 show the SF and the reduced normalizations as functions of the potential radius  $r_n$  (with  $a_n=0.68$  fm,  $V_{ns}=6.6$  MeV), of the diffuseness  $a_n$  (with  $r_n=1.23$  fm,  $V_{ns}=6.6$  MeV), and the spin-orbit potential depth  $V_{ns}$  (with  $r_n=1.23$  fm,  $a_n=0.68$  fm). While the  $\Lambda_{IJ}$  remain almost constant, the  $S_{IJ}$  depend rather sensitively on  $r_n$  and  $a_n$  and somewhat less on  $V_{ns}$ . These results agree with similar but less extensive investigations for  $^{139}\text{Ba}$  and  $^{93}\text{Zr}$  by other authors.<sup>39,50</sup> The approximate linear slope of the  $S_{IJ}$  on a semilogarithmic plot is expected according to analytical solutions of the bound state Schrödinger equations.<sup>51</sup> This was also confirmed by other authors for various other cases.<sup>39-41</sup>

The effect of the wave functions reaching to the nuclear interior was studied in the usual way by introducing a lower cutoff radius in Eq. (2). The worst cases occur at the highest incident energies.

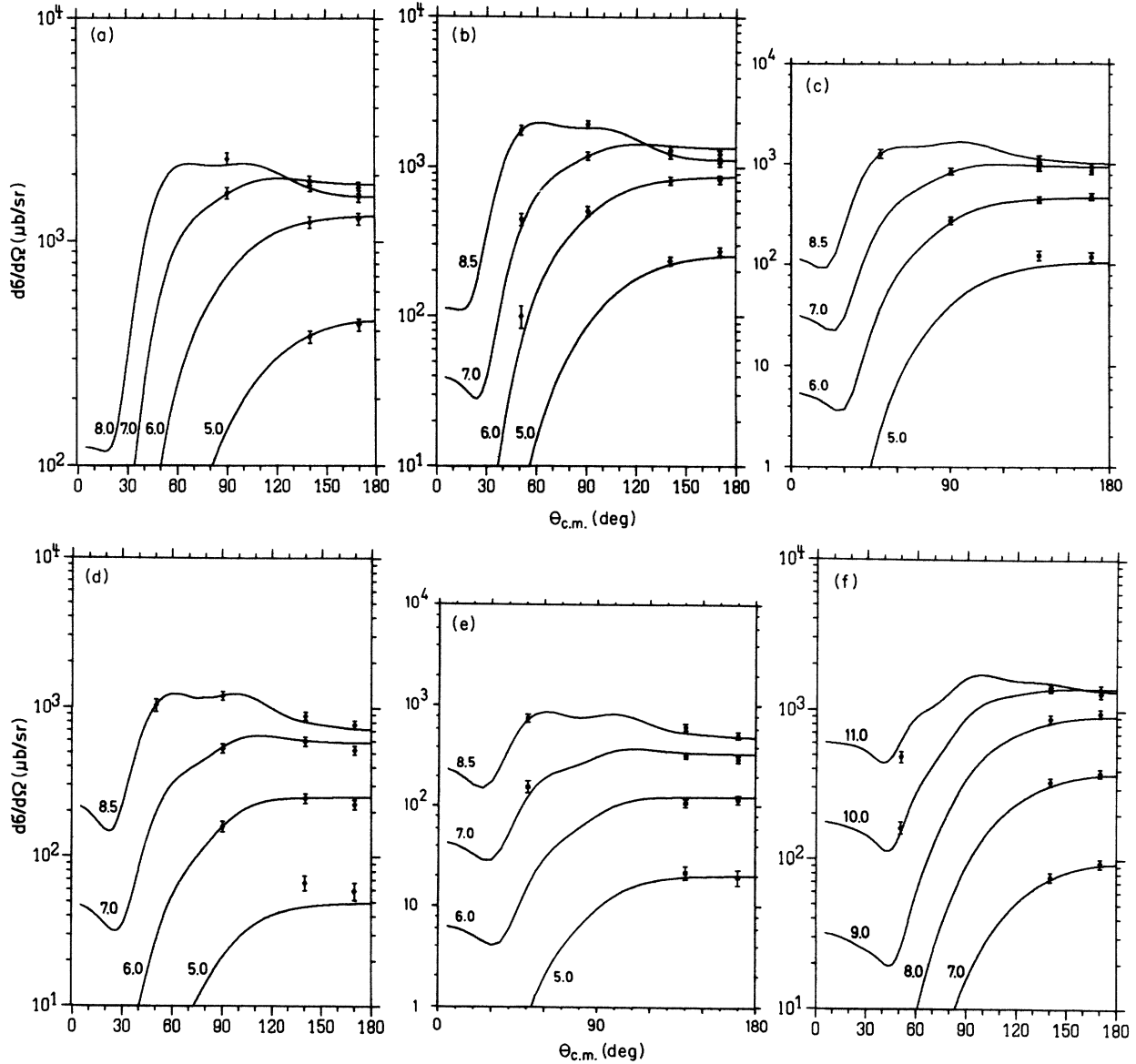


FIG. 3. Angular distributions of the  $(d, p)$  reactions. The solid curves are calculated with the DWBA code *dwuck* using the potential parameters in Table III and are adjusted by the spectroscopic factors in Table IV. (a)  $^{124}\text{Sn}(d, p)^{125}\text{Sn}$  ( $E_x = 2.788$  MeV,  $J^\pi = \frac{7}{2}^-$ ); (b)  $^{130}\text{Te}(d, p)^{131}\text{Te}$  ( $E_x = 2.279$  MeV,  $J^\pi = \frac{7}{2}^-$ ); (c)  $^{138}\text{Ba}(d, p)^{139}\text{Ba}$  ( $E_x = 0.0$  MeV,  $J^\pi = \frac{7}{2}^-$ ); (d)  $^{140}\text{Ce}(d, p)^{141}\text{Ce}$  ( $E_x = 0.0$  MeV,  $J^\pi = \frac{7}{2}^-$ ); (e)  $^{142}\text{Nd}(d, p)^{143}\text{Nd}$  ( $E_x = 0.0$  MeV,  $J^\pi = \frac{7}{2}^-$ ); (f)  $^{208}\text{Pb}(d, p)^{209}\text{Pb}$  ( $E_x = 0.0$  MeV,  $J^\pi = \frac{9}{2}^+$ ).

But even there, with cutoff radii of 1 fm greater than the radii of the appropriate neutron potentials, the DWBA cross sections changed, with the exception of one state, by less than 12%. The uncertainties inherent in DWBA calculations done with the zero-range approximation and local scattering potentials are considerably reduced at low energies of incoming and outgoing particles.<sup>3, 52</sup> According to the estimates of various authors<sup>3, 4, 53, 54</sup> a correction for finite-range interaction would decrease

the spectroscopic factors by only 4 to 7%. This statement could be proved true by calculations in the local energy approximation<sup>55</sup> with *DWUCK* for the states with  $E_x = 0.0$  MeV,  $J^\pi = \frac{7}{2}^-$  and  $E_x = 0.666$  MeV,  $J^\pi = \frac{3}{2}^-$  in  $^{141}\text{Ce}$  and  $E_x = 0.0$  MeV,  $J^\pi = \frac{9}{2}^+$  and  $E_x = 2.036$  MeV,  $J^\pi = \frac{1}{2}^+$  in  $^{209}\text{Pb}$ . The SF of these states decreased by the amount of 4 to 6%. A correction due to the nonlocality of the scattering potentials increased the same SF by less than 1% which is also in agreement with the results of other

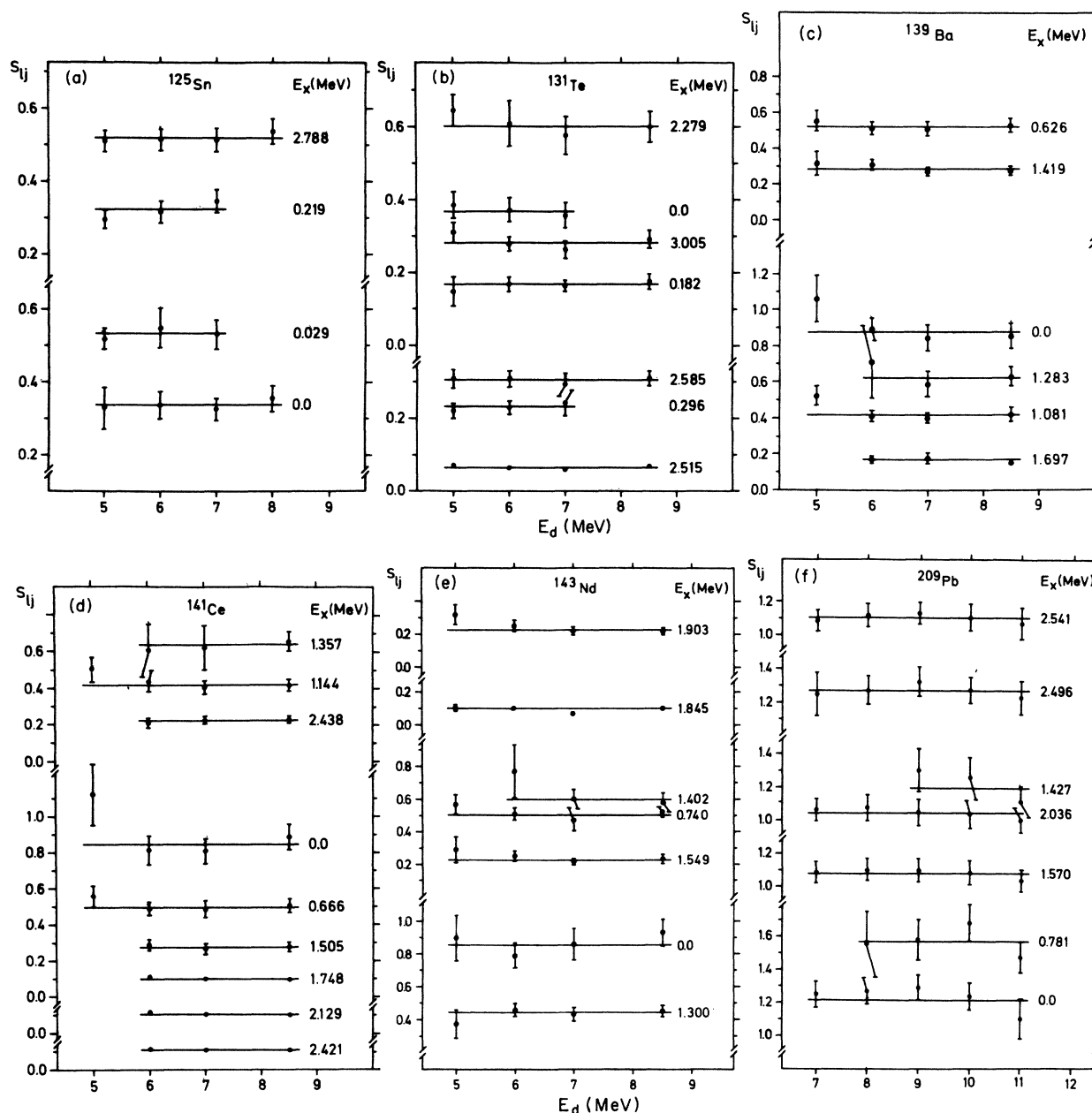


FIG. 4. Spectroscopic factors versus incident deuteron energies. The errors in the  $S_{ij}$  are directly obtained from the errors of the  $\Lambda_{ij}$  as discussed in the text.

TABLE V. Sets of parameters of the elastic deuteron scattering on  $^{130}\text{Te}$ . Set A was given by Perey and Perey (Ref. 49) and used by Graue *et al.* (Ref. 38). Sets B and C were obtained by fits to the measured elastic deuteron cross sections. The difference of the  $\chi^2$  in the fits with B and C is less than 3%.

Set	$V_R$ (MeV)	$W_D$ (MeV)	$V_S$ (MeV)	$r_R$ (fm)	$r_I$ (fm)	$r_S$ (fm)	$r_C$ (fm)	$a_R$ (fm)	$a_I$ (fm)	$a_S$ (fm)
A	100.0-0.22 $E$	15.25	...	1.15	1.34	...	1.3	0.81	0.68	...
B	116.4-0.5 $E$	20.2-0.25 $E$	7.8	1.200	1.350	1.16	1.20	0.833	0.687	0.84
C	131.3-0.5 $E$	13.5-0.25 $E$	9.9	1.120	1.350	1.16	1.20	0.860	0.760	0.84

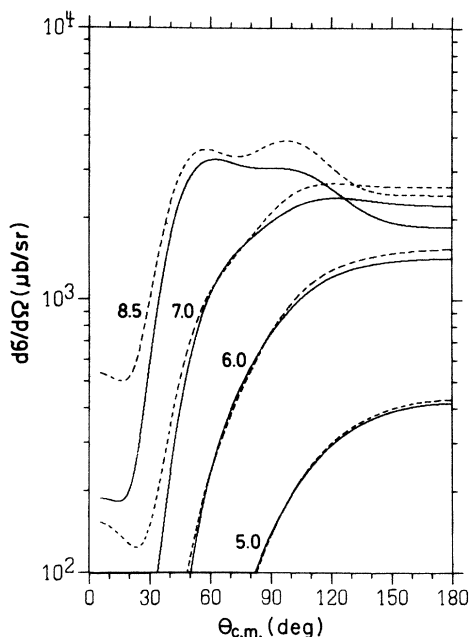


FIG. 5. Angular distributions of the reaction  $^{130}\text{Te}(d,p)^{131}\text{Te}$  ( $E_x = 2.279$  MeV,  $J^\pi = \frac{7}{2}^-$ ) calculated with the deuteron potential A in Table V (dotted lines) and the deuteron potential of the best fit to the measured elastic deuteron scattering data (cf. Table III).

authors. As both corrections are small and their theoretical uncertainties are in the same range they were not taken into account.

Another possible disturbing effect is the polarization of the deuteron by the Coulomb field of the target nucleus. In accordance with previous investigations<sup>4,39</sup> one can estimate the corrections due to this effect. At the lowest incident energies, *i.e.*, at 5.0 and 7.0 MeV, respectively, the SF would be 5% smaller, while at the highest deuteron energies of our experiments the influence is negligible.

Independent of the energies of the incoming and outgoing particles is the uncertainty of the factor  $D_0$  which can be calculated from the  $p$ - $n$  interaction and the internal wave function of the deuteron. Assuming a Hulthén function the literature values of  $D_0^2$  in units of  $10^4$  MeV<sup>2</sup> fm<sup>3</sup> vary from 1.50 to 1.65 (Refs. 47 and 56–58). Goldfarb<sup>57</sup> recommends 1.58 but does not exclude the value<sup>47</sup> of 1.53 used in this work.

Since the most important points mentioned give uncertainties with the same sign, the reduced normalizations (cf. Table IV) may decrease by about 15% if all the uncertainties take their maximum values, which is not probable.

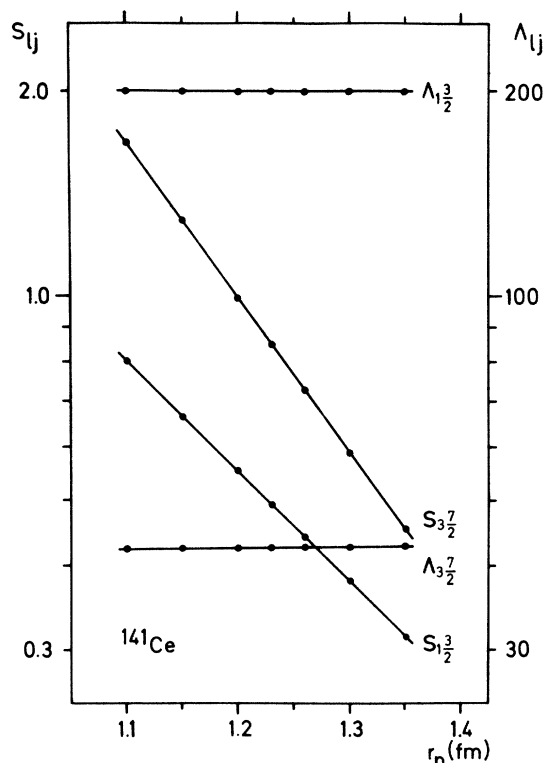


FIG. 6. Dependence of the spectroscopic factors  $S_{ij}$  and the reduced normalizations  $\Lambda_{ij}$  for the states ( $E_x = 0.0$  MeV,  $J^\pi = \frac{7}{2}^-$ ) and ( $E_x = 0.666$  MeV,  $J^\pi = \frac{3}{2}^-$ ) in  $^{141}\text{Ce}$  on the neutron potential radius parameter  $r_n$  (diffuseness  $a_n = 0.68$  fm, depth of the spin-orbit potential  $V_{ns} = 6.6$  MeV).

## VII. DISCUSSION

Finally, it is interesting to compare the results of this work with the results of other similar experiments. Unfortunately, only a few authors have reported reduced normalizations  $\Lambda_{ij}$ , and thus a comparison of results is not easy. Two important works should be mentioned: an investigation of  $^{139}\text{Ba}$  by Rapaport and Kerman<sup>39</sup> and of  $^{141}\text{Ce}$ ,  $^{143}\text{Nd}$ , and other nuclei by Norton *et al.*<sup>40</sup> The values of Refs. 39 and 40 for the first three states of the nuclei of interest agree with our values within  $\pm 25\%$ , *i.e.*, within the errors quoted. The larger disagreement for the higher excited states is probably due to some problems with energy resolution in the work of Ref. 40.

Summing up, we have found that one can extract reliable reduced normalizations at energies in the vicinity of the Coulomb barrier and slightly above. This quasi-Coulomb stripping needs, however,

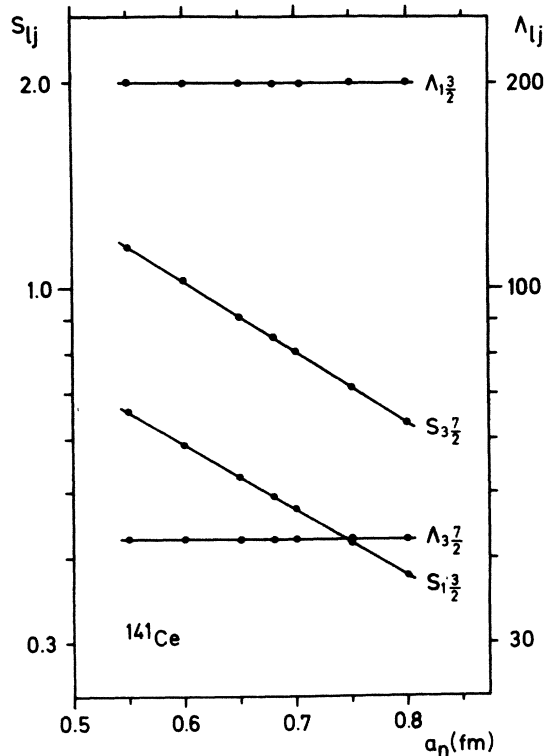


FIG. 7. Dependence of the spectroscopic factors  $S_{ij}$  and the reduced normalizations  $\Lambda_{ij}$  for the states ( $E_x = 0.0$  MeV,  $J^\pi = \frac{7}{2}^-$ ) and ( $E_x = 0.666$  MeV,  $J^\pi = \frac{3}{2}^-$ ) in  $^{141}\text{Ce}$  on the neutron potential diffuseness  $a_n$  (radius parameter  $r_n = 1.23$  fm, depth of the spin-orbit potential  $V_{ns} = 6.6$  MeV).

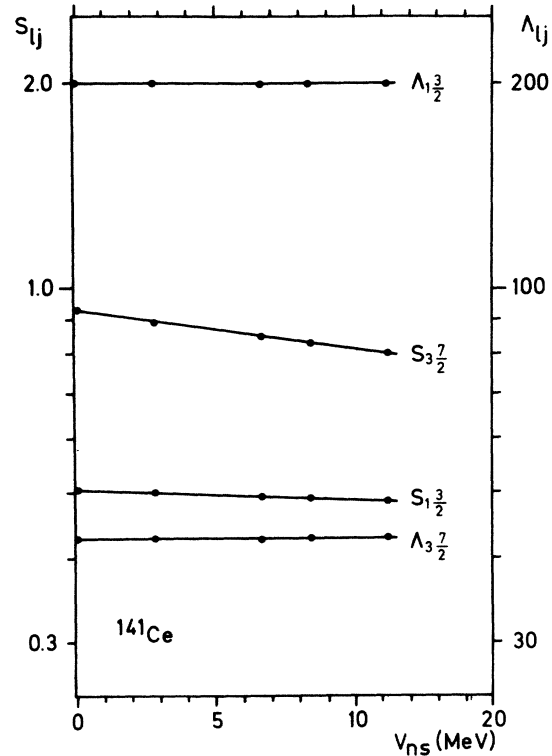


FIG. 8. Dependence of the spectroscopic factors  $S_{ij}$  and the reduced normalizations  $\Lambda_{ij}$  for the states ( $E_x = 0.0$  MeV,  $J^\pi = \frac{7}{2}^-$ ) and ( $E_x = 0.666$  MeV,  $J^\pi = \frac{3}{2}^-$ ) in  $^{141}\text{Ce}$  on the depth of the neutron spin-orbit potential  $V_{ns}$  (radius parameter  $r_n = 1.23$  fm, diffuseness  $a_n = 0.68$  fm).

careful attention to the fitting of the elastic scattering data in order to obtain appropriate optical potentials. These were found to be pinpointed best by the backward deuteron scattering. We conclude that quasi-Coulomb stripping, as opposed to both high energy and pure Coulomb stripping, seems to have valid applicability.

#### ACKNOWLEDGMENTS

We thank Professor Dr. K. H. Lauterjung for providing excellent research conditions in his institute. We appreciate the extraordinary assistance of the staff in running the accelerator and making instruments and targets.

\*Present address: INTERATOM, Bergisch Gladbach, Germany.

†Present address: Institut für Experimentalphysik III, Ruhr-Universität Bochum, Bochum, Germany.

‡Supported by Bundesministerium für Forschung und Technologie der Bundesrepublik Deutschland.

<sup>1</sup>R. H. Bassel, R. M. Drisko, and G. R. Satchler, *Phys. Rev.* **136**, B960 (1964).

<sup>2</sup>M. E. Cage, A. J. Cole, and G. J. Pyle, *Nucl. Phys.* **A201**, 418 (1973).

<sup>3</sup>L. J. B. Goldfarb, *Nucl. Phys.* **72**, 537 (1965); in *Lectures in Theoretical Physics* (Univ. of Colorado Press, Boulder, 1966), Vol. VIIIc.

<sup>4</sup>F. P. Gibson and A. K. Kerman, *Phys. Rev.* **145**, 758

(1966).

<sup>5</sup>M. Dost and W. R. Hering, *Phys. Lett.* **26B**, 443 (1968).

<sup>6</sup>W. R. Smith, *Nucl. Phys.* **72**, 593 (1965).

<sup>7</sup>P. von Brentano, M. Dost, and H. L. Harney, in *Theory of Nuclear Structure, Trieste Lectures, 1969* (IAEA, Vienna, 1970).

<sup>8</sup>P. Richard, C. F. Moore, J. A. Becker, and J. D. Fox, *Phys. Rev.* **145**, 971 (1966).

<sup>9</sup>R. Arking, R. N. Boyd, J. C. Lombardi, A. B. Robbins, and B. Gonsior, *Nucl. Phys.* **A155**, 480 (1970).

<sup>10</sup>S. Darmodjo, R. D. Alders, D. G. Martin, P. Dyer, S. Ali, and S. A. A. Zaidi, *Phys. Rev. C* **4**, 3, 672 (1971).

<sup>11</sup>J. L. Foster, Jr., P. J. Riley, and C. F. Moore, *Phys.*

- Rev. 175, 1498 (1968).
- <sup>12</sup>J. Burde, G. Engler, A. Ginsberg, A. A. Jaffe, A. Marinov, and L. Birstein, Nucl. Phys. A141, 375 (1970).
- <sup>13</sup>H. R. Hiddleston, C. K. Hollas, V. D. Mistry, and P. J. Riley, Phys. Rev. C 3, 905 (1971).
- <sup>14</sup>M. Roth, Ph.D. thesis, Universität zu Köln, 1972 (unpublished).
- <sup>15</sup>H. Seitz, D. Rieck, P. von Brentano, J. P. Wurm, and S. A. A. Zaidi, Nucl. Phys. A140, 673 (1970).
- <sup>16</sup>N. Williams, G. C. Morrison, J. A. Nolen, Jr., Z. Vager, and D. von Ehrenstein, Phys. Rev. C 2, 1539 (1970).
- <sup>17</sup>G. Zöllner, Diplomarbeit, University of Erlangen-Nürnberg, 1973 (unpublished).
- <sup>18</sup>L. Veaser and W. Haerberli, Nucl. Phys. A115, 172 (1968).
- <sup>19</sup>N. Marquardt, P. Rauser, P. von Brentano, J. P. Wurm, and S. A. A. Zaidi, Nucl. Phys. A177, 33 (1971).
- <sup>20</sup>P. Schulze-Döbold, Diplomarbeit, University of Erlangen-Nürnberg, 1971 (unpublished).
- <sup>21</sup>G. Clausnitzer, R. Fleischmann, G. Graw, D. Proetel, and J. P. Wurm, Nucl. Phys. A106, 99 (1968).
- <sup>22</sup>E. Grosse, K. Melchior, H. Seitz, P. von Brentano, J. P. Wurm, and S. A. A. Zaidi, Nucl. Phys. A142, 345 (1970).
- <sup>23</sup>W. R. Wharton, P. von Brentano, W. K. Dawson, and P. Richard, Phys. Rev. 176, 1424 (1968).
- <sup>24</sup>J. G. Cramer (private communication).
- <sup>25</sup>E. J. Schneid, A. Prakash, and B. L. Cohen, Phys. Rev. 156, 1316 (1967).
- <sup>26</sup>R. K. Jolly, Phys. Rev. 136, B638 (1964).
- <sup>27</sup>D. von Ehrenstein, G. C. Morrison, J. A. Nolen, Jr., and N. Williams, Phys. Rev. C 1, 2066 (1970).
- <sup>28</sup>S. S. Ipson, W. Booth, and J. G. Haigh, Nucl. Phys. A206, 114 (1973); W. Booth, S. Wilson, and S. S. Ipson, *ibid.* A238, 301 (1975).
- <sup>29</sup>C. A. Wiedner, A. Heusler, J. Solf, and J. P. Wurm, Nucl. Phys. A103, 433 (1967).
- <sup>30</sup>P. R. Christensen, B. Herskind, R. R. Borchers, and L. Westgaard, Nucl. Phys. A131, 267 (1969).
- <sup>31</sup>G. Muehlechner, A. S. Poltorak, W. G. Parkinson, and R. H. Bassel, Phys. Rev. 159, 1039 (1967).
- <sup>32</sup>C. Ellegaard, J. Kantele, and P. Vedelsby, Nucl. Phys. A129, 113 (1969).
- <sup>33</sup>R. F. Casten, E. Cosman, E. R. Flynn, O. Hausen, P. W. Keaton, Jr., N. Stein, and R. Stock, Nucl. Phys. A202, 161 (1973).
- <sup>34</sup>D. P. Powell, P. J. Dallimore, and W. F. Davidson, Australian National University, Report No. ANU-P/511, 1971 (unpublished).
- <sup>35</sup>A. F. Jeans, W. Darcey, W. G. Davies, K. N. Jones, and P. K. Smith, Nucl. Phys. A128, 224 (1969).
- <sup>36</sup>J. J. van der Merve and G. Heymann, Z. Phys. 220, 130 (1969).
- <sup>37</sup>P. L. Carson and L. C. McIntyre, Jr., Nucl. Phys. A198, 289 (1972).
- <sup>38</sup>A. Graue, E. Jastad, J. R. Lien, P. Torvud, and W. H. Moore, Nucl. Phys. A103, 209 (1967).
- <sup>39</sup>J. Rapaport and A. K. Kerman, Nucl. Phys. A119, 641 (1968).
- <sup>40</sup>G. A. Norton, H. J. Hausmann, J. J. Kent, J. F. Morgan, and R. G. Seyler, Phys. Rev. Lett. 31, 769 (1973); Phys. Rev. C 9, 1594 (1974).
- <sup>41</sup>M. Dost and W. R. Hering, Phys. Lett. 19, 488 (1965); Z. Naturforschung 21a, 1015 (1966); M. Dost, W. R. Hering, and W. R. Smith, Nucl. Phys. A93, 357 (1967).
- <sup>42</sup>G. M. Crawley, B. V. Narisimha Rao, and D. L. Powell, Nucl. Phys. A112, 223 (1968).
- <sup>43</sup>R. Bangert, Jahresbericht 1968/69 des Instituts für Kernphysik der Universität zu Köln, Report No. BMBW-FB K 71-09 (unpublished).
- <sup>44</sup>H. R. Collard and R. Hofstadter, *Kernradien, Landolt-Börnstein: Numerical Data and Functional Relationships* (Springer, Berlin, 1967), New Series, Group I, Vol. 2.
- <sup>45</sup>B. Steinmetz, Ph.D. thesis, Universität zu Köln, 1973 (unpublished); Jahresbericht 1970/71 des Instituts für Kernphysik der Universität zu Köln, Report No. BMFT-FB K 73-02 (unpublished).
- <sup>46</sup>W. Fitz, Computer Codemom3, University of Hamburg, private communication.
- <sup>47</sup>P. D. Kunz, University of Colorado, Boulder, Colorado, Computer Code DWUCK and Internal Reports Nos. C00-535-606 and C00-535-613 (unpublished).
- <sup>48</sup>R. G. Clarkson and H. L. Harney, Computer Code BETTINA and Description of Program BETTINA, Univ. of Oregon, Lab Report No. RLO-1925-48, 1971 (unpublished).
- <sup>49</sup>C. Perey and F. G. Perey, Phys. Rev. 132, 755 (1963).
- <sup>50</sup>J. J. Kent, J. F. Morgan, and R. G. Seyler, Nucl. Phys. A197, 177 (1972).
- <sup>51</sup>S. Flügge, *Practical Quantum Mechanics* (Springer-Verlag, Heidelberg-New York, 1971), Vol. I.
- <sup>52</sup>N. Austern, *Direct Nuclear Reaction Theories* (Wiley Interscience, New York, 1970).
- <sup>53</sup>L. J. B. Goldfarb and E. Parry, Nucl. Phys. A116, 309 (1968).
- <sup>54</sup>W. R. Hering, H. Becker, C. A. Wiedner, and W. J. Thompson, Nucl. Phys. A151, 33 (1970).
- <sup>55</sup>P. J. A. Buttle and L. J. B. Goldfarb, Proc. Phys. Soc. 83, 701 (1964).
- <sup>56</sup>R. H. Bassel, R. M. Drisco, and G. R. Satchler, ORNL Report No. ORNL-3240, 1962 (unpublished).
- <sup>57</sup>L. J. B. Goldfarb, Phys. Lett. 24B, 264 (1967).
- <sup>58</sup>W. J. Thompson and W. R. Hering, Phys. Rev. Lett. 27, 1457 (1971).